Experimental Study of Heating Mechanism in Low-pressure Microwave Plasmas

Tibor TEREBESSY, Jozef KUDELA* and Masashi KANDO

Abstract

In this work, we present an experimental study focused on the hot electrons in low-pressure large-area microwave discharges. At gas pressures below about 50 mTorr, a flux of hot-electrons directed away from the waveguiding plasma-dielectric interface has been observed. Energies of these electrons attain values of some 60 eV and they are believed to be originating from the resonantly enhanced electric field region localized near the dielectric. The hot-electron flux appears to play a significant role in the discharge heating mechanism, which is demonstrated by plasma parameter profiles. In the profiles of slightly overdense discharges, a localized hot-electron region has been observed near the dielectric in the place of critical plasma density. The existence of both presented phenomena, the hot-electron flux and the localized hot electrons is explained on the basis of the transit-time heating in the resonantly enhanced electric field. The presented experimental results provide an evidence that the plasma resonance region plays an active role in the maintenance of low-pressure microwave discharges.

1. Introduction

Microwave discharges are widely used in industrial applications. Recently, increasing attention has been paid to the so-called large-area surface-wave (SW) plasma sources [1-5]. These sources work without the use of static magnetic fields and produce plasmas of high densities ($>10^{11}$ cm^{-3}) over large areas, which makes them attractive for the industrial applications. The plasma is produced as a result of energy absorption of an electromagnetic wave propagating along the plasma-dielectric interface. At low gas pressures, where the electron-neutral collision frequency is much lower than the applied field frequency, the main mechanism of the energy absorption turns out to be collisionless rather than the conventional Joule heating. For the SW-discharges sustained in thin cylindrical dielectric tubes [6], this phenomenon has been theoretically described by Aliev *et al.*[7-9] as follows: In a cylindrical SW-plasma column, due to the radial plasma inhomogeneity, a region with enhanced radial electric field exists near the plasma column boundary where the local plasma frequency equals the applied frequency. By quasi-linear wave-particle interactions, this enhanced field accelerates the electrons down the plasma density gradient (to the wall), which results in the formation of a hot tail in the electron energy distribution function. These hot electrons are reflected back from the negatively charged wall and sustain the discharge.

Obviously, the region of the resonantly enhanced electric field near the plasma-dielectric boundary is expected to exist also in the large-area SW plasmas, which has already been discussed in a few works [10-13]. Taking into account the above-mentioned theory [7-9], in our work, we have focused on the experimental observation of hot electrons and their role in discharge heating.

In this paper we present an overview of our recent results [14,15]. The paper is organized as follows: Section 2 describes the experimental apparatus. In section 3.1, the observation of a hot-electron flux directed away from the waveguiding plasma-dielectric interface is presented. The presence of the hot-electron flux is supported also by the plasma parameter profiles shown in section 3.2. Section 3.3 presents the detection of hot electrons localized in the plasma resonance region near the dielectric. The presented experimental results are supported by the explanation based on the transit-time heating in section 4. Finally, a summary with the impact of the observed phenomena on the processing is given in section 5.

Graduate School of Electronic Science and Technology, Shizuoka University, Johoku 3-5-1, Hamamatsu 432-8561, Japan
* Satellite Venture Business Laboratory, Shizuoka University, Johoku 3-5-1, Hamamatsu 432-8561, Japan

2. Description of the Plasma Source

The experiments were carried out in argon gas in a large-area microwave planar plasma source [5,16] schematically shown in **Fig. 1**. Vacuum part consists of a cylindrical chamber with 312-mm diameter and 350-mm height. 2.45-GHz microwaves are coupled to the plasma chamber through a 15-mm-thick quartz window by a fully azimuthally symmetrical microwave applicator. The applicator is a tunable cylindrical cavity designed for the TM_{011}-mode with an annular slot at its bottom wall. The cavity is made of copper cylinder with the inner diameter of 110 mm. The bottom wall of the cavity is a 5-mm-thick and 90-mm-diameter disk, which together with the cylindrical body of the cavity forms an annular slot with 10-mm width and 110-mm outer diameter.

In the experiments, two Langmuir probes were used. The probe-1 was inserted into the chamber through a side-port in a 100-mm distance under the quartz plate and the probe-2 through a bottom-port along the side-wall as shown in **Fig.1**. Both probes were movable in the axial and azimuthal directions.

3. Experimental Results

3.1. Hot-electron Flux in Low-pressure Discharges

The existence of a directed electron flux in the discharges was investigated firstly by rotating the probe-1 (**Fig. 1**) with an L-shape-bent probe tip (**Fig. 2**) around the probe axis. By this technique, a probe tip with length much larger than diameter, in different orientations, exhibits different surfaces to the predicted electron flux. Consequently, this should lead to the changes in probe characteristics. In the

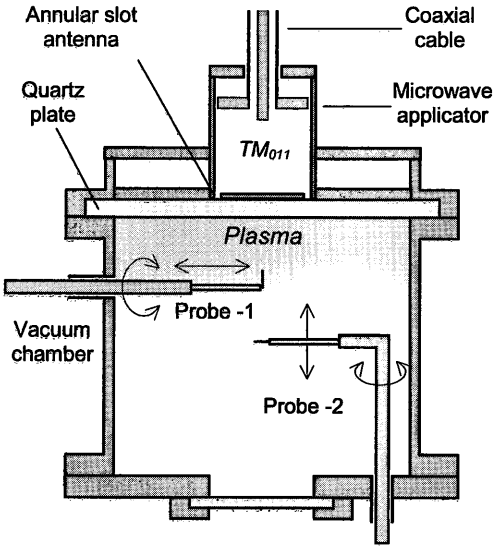

Fig.1 Schematic view of the plasma source.

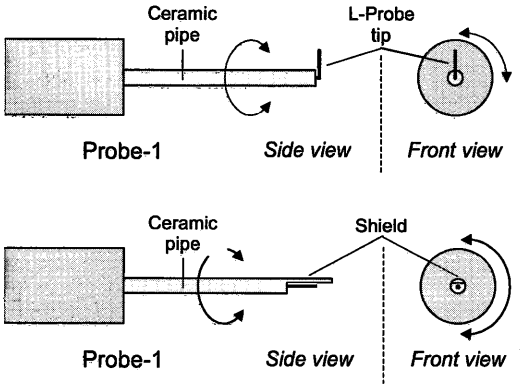

Fig.2 Details of the L-shape-bent and one-side-shielded probe tips of the probe-1 used for the observation of the hot-electron flux from the plasma-dielectric interface.

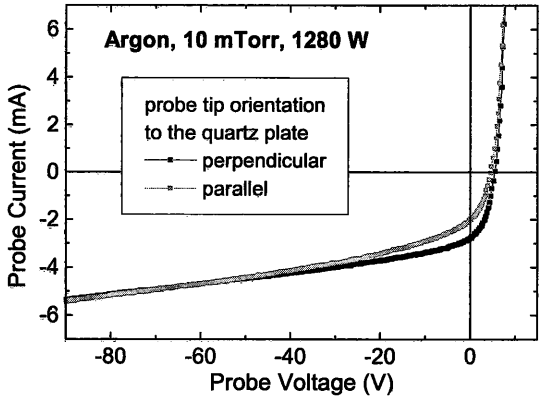

Fig.3 Part of probe characteristics measured at two different orientations of the L-shape-bent probe tip indicating the presence of hot-electron flux from the region near the quartz plate in a 10 mTorr argon discharge sustained by 1280 W. Probe was placed on chamber axis 100 mm under the quartz plate.

experiment, an 8-mm-long probe tip made of 0.4-mm-diameter tungsten wire was used. Measurements for the tip in two orientations, parallel and perpendicular to the quartz plate, placed on chamber axis 100 mm under the quartz in a 10 mTorr argon discharge are shown in **Fig. 3**. As it can be seen from the figure, deep in the ion saturation current region ($V_p \leqq$ -50 V), both characteristics are identical with the fits [17] implying ion density $N_i = 1.9\times10^{12}$ cm^{-3}. However, a significant difference is observed in the remaining part of characteristics. The lower values of probe current $-I_p$ measured by the probe with tip parallel to the quartz plate confirm the presence of axial flux of hot electrons to the probe. The estimated flux current density is roughly 30 mA/cm^2. The difference in currents at probe biases as high as about -50V and the value of the space potential V_s = 12.6 V together suggest hot electron energies attaining some 60 eV. We believe that these hot electrons originate from the predicted resonantly enhanced electric field region localized near the quartz. To confirm the electron flux direction another probe was used. This probe had a straight, 4-mm-long, one-side-shielded probe tip with the radial distance between the shield and probe surface 0.8 mm (**Fig. 2**). As in the previous measurement, the probe was rotated into two positions, with the shield up and down, respectively. The presence of hot electrons in probe characteristic was observed when the shield was under the probe tip (**Fig. 4**). The effect of gas pressure, also seen in **Fig.4**, provides additional support for the phenomenon. With increasing gas pressure the presence of directed flux of hot electrons becomes weaker and above some 30-50 mTorr, in a 100-mm-distance from the quartz, it is no more detected. This occurs apparently due to the collisions with neutrals: the mean free path of hot electrons can be estimated as $\lambda_{mfp} = v_e / \nu_{en}$, where $v_e = (2Ee/me)^{1/2}$ is the electron velocity and $\nu_{en} = 3\times10^9 p$[Torr] is the electron-neutral collision frequency. Assuming the electrons with energies E_e = 60 eV, the estimated mean free paths are 306 mm at 5 mTorr, 153 mm at 10 mTorr, 76 mm at 20 mTorr and 31 mm at 50 mTorr, which is in reasonably good agreement with the experimental observations.

3.2. Axial Plasma Parameter Profiles

It is reasonable to expect that the interaction of the hot electron flux with the neutral gas should affect the shapes of axial plasma parameter profiles. The profiles were measured by the probe-2 (**Fig 1**) with a conventional cylindrical probe tip. The probe was moved axially along the chamber axis to a minimum distance 10 mm from the quartz plate. First, the ion saturation current profiles (V_p = -50 V) measured for pressures ranging from 5 to 200 mTorr are presented in normalized forms in **Fig. 5**. It should be noted that the ion saturation current profiles, quantitatively, do not exactly correspond with the plasma density distributions due to axial variations of the space potential and the effective electron temperature, which will be shown below. However, for illustrative purposes, they provide sufficient information about the plasma density changes. At 200 mTorr, the profile exhibits maximum at the nearest measured point to the quartz plate and a relatively steep exponential-like decay away from it. At lower pressure, 100 mTorr, this decay becomes less steep and, at 50 mTorr, profile with a peak in the vicinity of the quartz is observed. With further decrease of pressure, the peak becomes wider and moves away from the quartz. Between 50 and 5 mTorr, the maximum values of ion

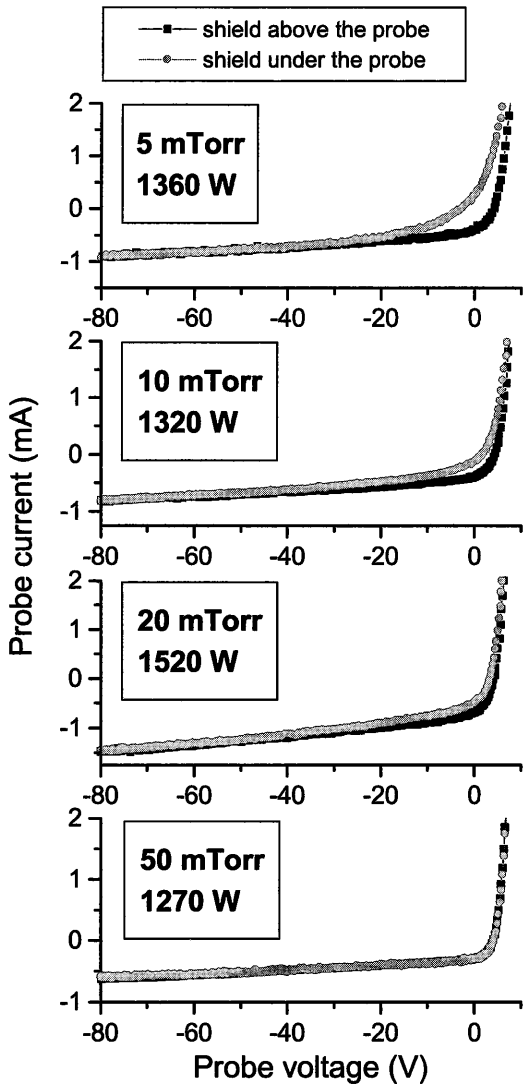

Fig.4 Part of probe characteristics measured at different gas pressures with the shield positioned above and under the probe tip. Probe was placed on chamber axis 100 mm under the quartz plate.

saturation current are measured in the axial positions of about 20 to 50 mm from the quartz. Considering skin depth for the applied electromagnetic field in these discharges being only a few millimeters ($\lambda_{sk} = 5.3$ mm at $N_e = 10^{12}$ cm^{-3}), such profiles support the assumption of plasma heating by the hot electron flux. To justify the profiles, complete probe characteristics were measured and analyzed for different probe positions. Figure 6 shows the actual variation of the ion density along with the temperature of Maxwellian electrons (determined from the linear part of $\ln I_e$-V curves) for pressures 50 and 10 mTorr. The temperature exhibits decreasing profile with stabilized values in distances larger than mean free path of hot electrons.

In view of the above observations, three distinctive space regions can be recognized in the axial direction. Starting from the quartz plate, there is the region of spatially localized enhanced electric field, where hot electrons are generated. Then the region follows, in which the hot electrons lose their energy. This region exhibits enhanced plasma density and decaying electron temperature. Finally, in a distance larger than the hot electron mean free path, the region of thermalised

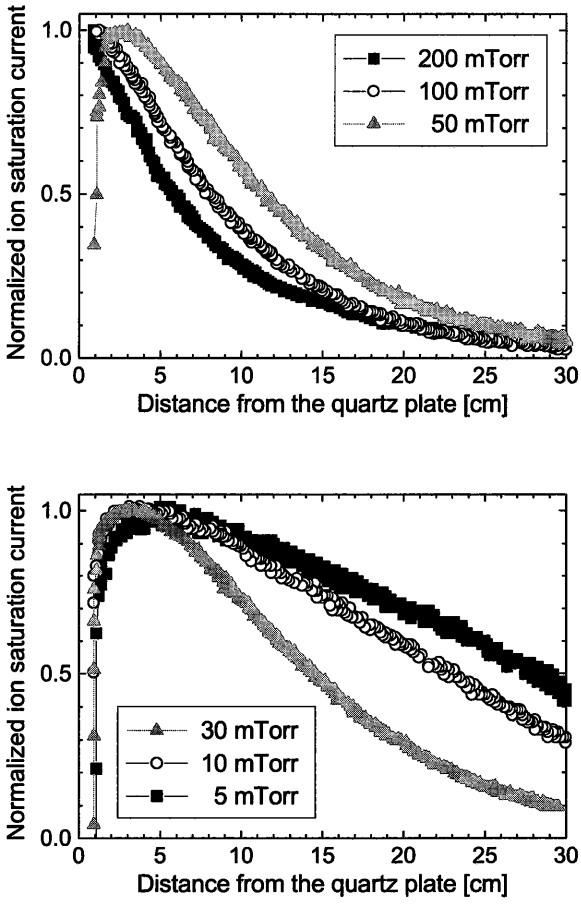

Fig.5 Normalized axial profiles of ion saturation current measured on the chamber axis in argon discharges sustained at different gas pressures.

diffusive plasma exists.

3.3. Localized Region of Hot Electrons

The axial plasma parameter profiles at lower gas pressures, typically under 3 mTorr, exhibit different behavior than the ones mentioned in the preceding section. **Figure 7** shows a probe current profile measured at 2.7 mTorr on the chamber axis at the probe bias $V_p = -50$ V. As it can be seen in the figure, a trough of the probe current with about 0.5-cm-width is observed near the quartz plate. The trough is observed always at the same value of the probe current (measured at the same probe bias) and it disappears when the plasma source operates in the underdense-plasma conditions. Therefore, we believe that the trough is related to the plasma resonance region. As expected, the phenomenon can be observed also in the radial probe current profiles (**Fig. 8**). The influence of the probe bias on the axial profile shown in **Fig. 9** suggests the explanation for the local decrease in the probe current. Under the same discharge conditions, the depth of the trough increases with decreasing negative probe bias and the current in the minimum can even change the sign. Such a behavior indicates that the trough is caused by the current of hot electrons to the probe collected in the resonantly enhanced electric field region. Further decrease of the probe current to negative values in the vicinity of the quartz is due to hot electrons generated by the strong electric field at the interface. The assumption of the trough formation is justified by axial probe current

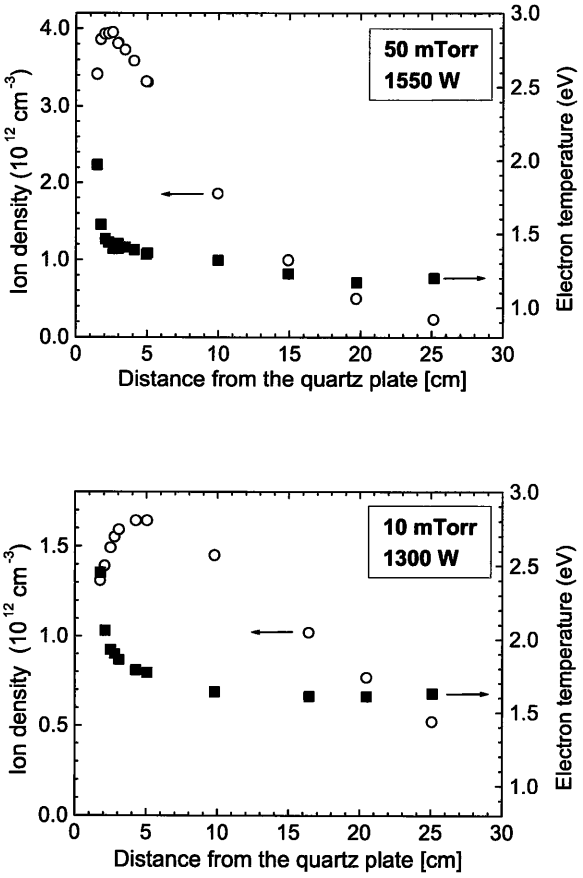

Fig.6 Axial profiles of ion density and electron temperature measured on the chamber axis in argon discharges sustained at 50 and 10 mTorr.

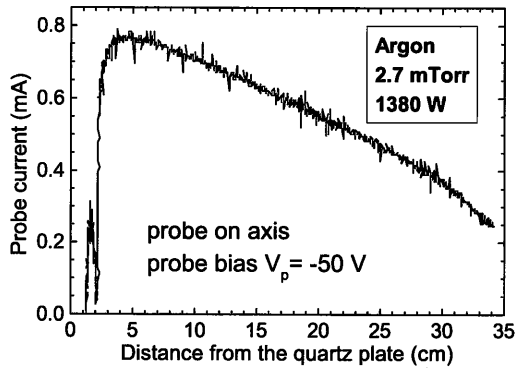

Fig.7 Typical axial probe current profile (V_p= -50V) observed on the chamber axis in argon discharges at very low gas pressures (< 3 mTorr).

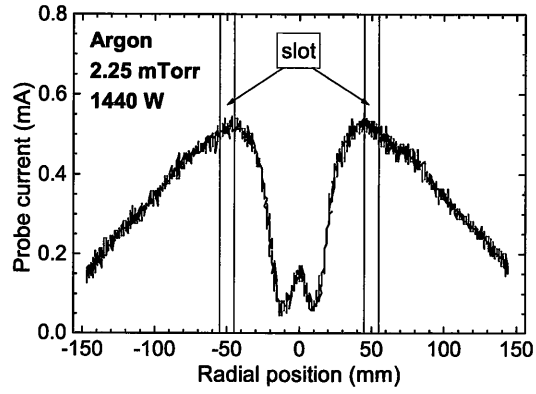

Fig.8 Radial probe current profile (V_p= -50V) measured 3 cm under the quartz plate in argon at 2.25 mTorr and 1440 W.

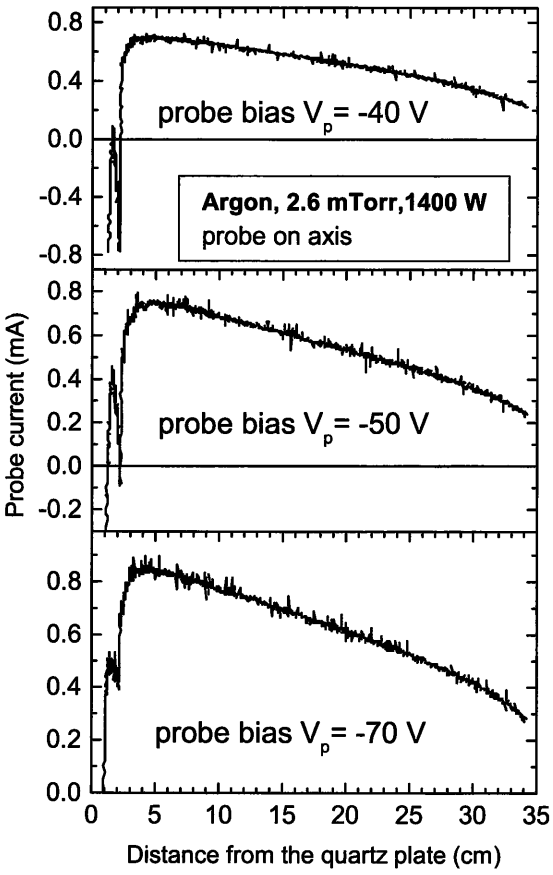

Fig. 9 Axial probe current profiles measured on the chamber axis in argon at 2.6 mTorr and 1400 W of absorbed microwave power at different probe biases.

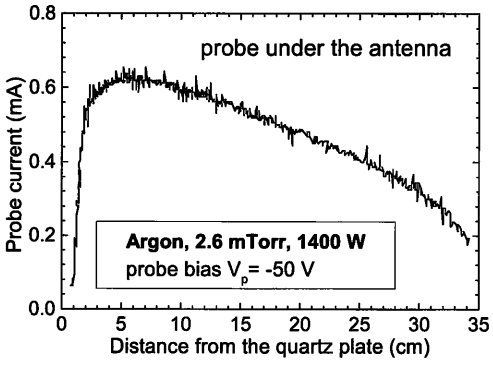

Fig.10 Axial probe current profile measured under the slot antenna in argon at 2.6 mTorr and 1400 W of absorbed microwave power. Probe bias V_p= -50V.

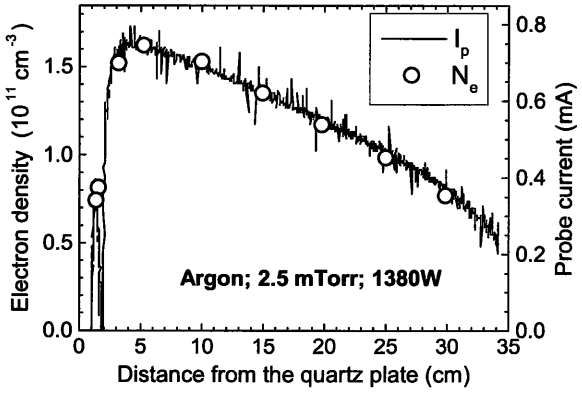

Fig.11 Axial electron density and probe current (V_p= -50V) profiles measured on the chamber axis in argon discharge at 2.5 mTorr and 1380 W.

profile measured under the slot antenna (**Fig.10**). As mentioned above, the hot electron generation is related to the perpendicular electric field component Ez, which is not expected to exist under the slot antenna. Indeed, the trough does not appear in the profile. Substantial experimental confirmation is provided by the measurement and complete evaluation of probe characteristics along the chamber axis. **Figure 11** shows the axial variation of the electron density *Ne* [18] and the probe current measured along the whole plasma chamber. As expected, the density profile is consistent with the probe current profile and the trough appears in the place where the density is close to the critical plasma density (7.4×10^{10} cm^{-3}). **Figure 12** provides more details on the spatial variations of plasma parameters over the plasma resonance region. The density profile exhibits a slight depletion in the plasma resonance region, which also contributes to the localized decrease of the probe current. However, as mentioned above, the main contribution to the formation of the probe current trough is due to hot electrons localized in the plasma resonance region. This is indicated by profiles of the floating potential V_f and the temperature of Maxwellian electrons T_e. The floating potential sharply decreases to less than -50 V in the plasma resonance region, while being about +5 V in the bulk plasma. This effect, along with the electron temperature profile, confirms the presence of a localized hot-electron region. Considering the value of the plasma potential V_s = 20 V and the fact that the trough is well observed up to about V_p = -50 V, the energy of the hot electrons is believed to be as high as 70 eV.

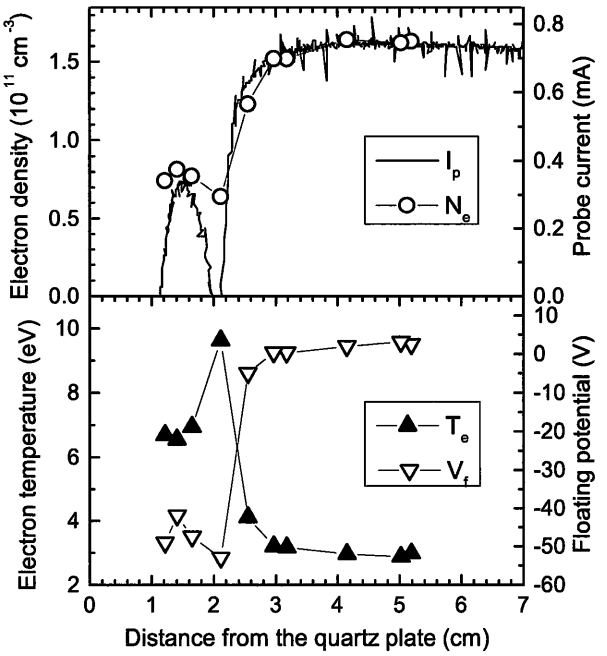

Fig.12 Axial plasma parameter and probe current (V_p= -50V) profiles measured on the chamber axis in argon discharge at 2.5 mTorr and 1380 W.

4. Discussion

The explanation of the hot-electron flux and the localized hot-electron region can be provided on the basis of the heating mechanism mentioned above [7-9] as follows: the electrons entering the plasma resonance region can gain energy from the enhanced high-frequency field and the efficiency of the power transfer depends on their transit time through the region. The energy gain is efficient only if the transit time (is short compared to the field period T (=*1/f*, where *f*=*2.45GHz* is the frequency of microwaves) and it reaches its maximum value at $\tau_{opt} \approx 0.7\,T/(4\pi)$ (**Fig. 13**) [7]. Under such a condition, the electrons are resonant (from the viewpoint of wave-particle energy transfer) and are accelerated out of the region resulting in hot-electron flux. However, if the transit time is comparable to the field period, the electron energy gain decreases since the electrons become non-resonant and are accelerated and afterwards decelerated by the reversing field when moving through the region of plasma resonance. Thus, the hot electrons "remain" localized in the plasma resonance region.

The considerations above can be strengthened by the estimation of the electron transit time through the plasma resonance region. The distribution of the resonantly enhanced electric field component E_z in the region (**Fig. 14**) can be expressed by the formula [19]:

$$E_z = \frac{E_0}{-(z - z_{res})/L + i(\nu_{eff}/\omega)}$$

Here E_0 is the electric field amplitude and L is the density scale-length at the resonance point z_{res}, ν_{eff} is the effective collision frequency and ω is the applied field frequency. The density scale-length is given as [9]:

$$L = \left(\frac{d \ln n}{dz} \Big|_{z=z_r} \right)^{-1}$$

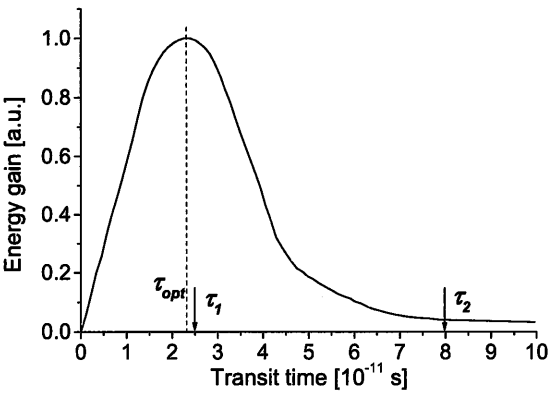

Fig.13 Efficiency of the energy transfer as a function of the electron transit-time through the plasma resonance region.

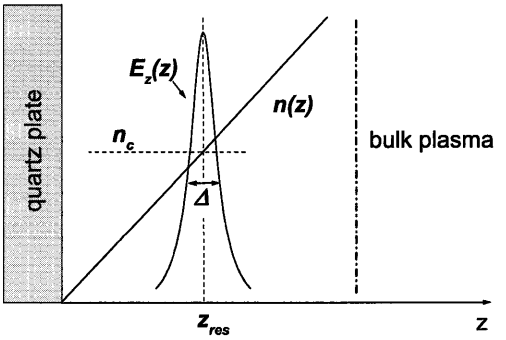

Fig.14 Enhancement of the electric field in an inhomogeneous plasma in the place of critical plasma density.

and, assuming a linear density profile near the quartz, it corresponds to the distance of the resonance region from the quartz. In the collisionless case, ν_{eff} is determined by the field convection caused by thermal electron motion effect given by the formula [9]:

$$\nu_{eff} = \omega\,(V_{Te}/\omega L)^{2/3}$$

where v_{Te} is the thermal velocity of electrons. The electron transit time through the region can be calculated by the formula:

$$\tau = \Delta / v_h$$

where v_h is the velocity of hot electrons and Δ is the width of the region defined as [9]:

$$\Delta = \frac{\nu_{eff}}{\omega} L$$

As mentioned in section 3.3, the efficiency of the energy transfer to the electrons in the resonance region strongly depends on the electron transit time through the region. This dependence is plotted in **Fig.13** [7]. In our experiments, the typical conditions for the strongest hot-electron flux (the strongest light emission and power absorption) are: p= 20 mTorr, L= 0.1 cm, T_e = 2eV, $v_h = 4.6\times10^8$ cm/s (corresponding to 60 eV), which gives $\nu_{eff} = 1.8\times10^9$ s^{-1} (determined by the field convection) and $\Delta = 1.1\times10^{-2}$ cm and, consequently, the electron transit time is estimated to $\tau_1 = 2.5\times10^{-11}$ s. This value corresponds well to the optimum transit time $\tau_{opt}\approx2.3\times10^{-11}$ s (see **Fig.13**). When the localized hot-electron region is observed the typical experimental conditions are as follows: p= 2.6 mTorr, L= 2.1 cm, T_e = 4 eV and v_h = 5×10^8 cm/s (corresponding to 70 eV). Under these conditions, the estimated parameters are: $\nu_{eff} = 2.9\times10^8$ s^{-1} and $\Delta = 4\times10^{-2}$ cm, which gives the electron transit time $\tau_2 = 8\times10^{-11}$ s. This value is comparable to the field period $T = 4\times10^{-10}$ s and it is about 3.5 times larger than the optimum time τ_{opt}, thus the condition for the effective power transfer to the electrons is not fulfilled. Indeed, under these experimental conditions, we do not observe the hot-electron flux.

5. Summary

An experimental study on hot electrons in low-pressure large-area microwave discharges has been presented. At gas pressures below about 50 mTorr, a flux of hot electrons directed away from the waveguiding plasma-dielectric interface was observed. These electrons are believed to be originating from the region of resonantly enhanced electric field near the dielectric. They contribute significantly to discharge heating, which was demonstrated by the axial plasma parameter profiles. At pressures below 3 mTorr, a trough in the probe current profiles was observed near the quartz plate. The trough appears in the place of critical plasma density and we believe that it is caused by the localized hot electrons generated in the resonantly enhanced electric field. The formation of both, the hot-electron flux and the localized hot-electron region is explained on the basis of the transit-time heating. The presented experimental results can be considered as an evidence that the plasma resonance region plays an active role for the heating mechanism in the low-pressure microwave discharges.

We believe that the phenomena may be an important factor in processing plasmas affecting the discharge chemistry in the volume plasma and on the processing surface as well. Particularly, the hot electron flux depositing the energy and charge on the processing surface may have a strong impact. This can be either positive or negative depending on the required process. Moreover, the occurrence of the hot-electron flux can also affect the discharge stability, which appears to be an issue for the large-area microwave discharges.

Acknowledgement

The authors are indebted to Prof. Yu. M. Aliev of Lebedev Physical Institute of Russian Academy of Sciences and Dr. D. Korzec of Microstructure Research Center of University of Wuppertal (Germany) for helpful discussions. This work was supported by a Grant-in-Aid for scientific Research (B)(2) from the Ministry of Education, Science, Sports and Culture of Government of Japan.

References

1) K. Komachi and S. Kobayashi: J. Microwave Power and Electromag. Energy, **24** (1989) 216

2) T. Kimura, Y. Yoshida and S. Mizuguchi: Jpn. J. Appl. Phys. **34** (1995) 1076

3) F. Werner, D. Korzec and J. Engemann: Plasma Sources Sci. Technol. **3** (1994) 473

4) M. Nagatsu, G. Xu, M. Yamage, M. Kanoh, H.Sugai: Jpn. J. Appl. Phys. **35** (1996) 341

5) I. Odrobina, J. Kudela and M. Kando: Plasma Sources Sci. Technol. **7** (1998) 238

6) M. Moisan, J. Margot and Z. Zakrzewski: High Density Plasma Sources, ed. O.A. Popov (Noyes Publication, Park Ridge, 1996), 191

7) Yu.M. Aliev, V.Yu. Bychenkov, A.V. Maximov, and H. Schluter: Plasma Sources Sci. Technol. **1** (1992) 126

8) Yu.M. Aliev, A.V. Maximov, U. Kortshagen, H. Schluter, and A. Shivarova: Phys. Rev. E **51** (1995) 6091

9) Yu. M. Aliev, H. Schluter, and A. Shivarova: Guided-Wave-Produced Plasmas (Springer-Verlag, Berlin, 2000) 206

10) E. Rauchle: J. Phys. IV France **8** (1998) 99

11) H. Sugai, I. Ghanashev and M. Nagatsu: Plasma Sources Sci. Technol. **7** (1998) 192

12) I. Ghanashev, H. Sugai, S. Morita, and N. Toyoda: Plasma Sources Sci. Technol. **8** (1999) 363

13) Y. Yasaka, D. Nozaki, K. Koga, M. Ando, T. Yamamoto, N. Goto, N. Ishii, and T. Morimoto: Jpn. J. Appl. Phys. **38** (1999) 4309

14) J. Kudela, T. Terebessy, and M. Kando: Appl. Phys. Lett. **76** (2000) 1249

15) T. Terebessy, M. Kando, and J. Kudela: Appl. Phys. Lett. **77** (2000) 2825

16) J. Kudela: Doctor thesis, Graduate School of Electronic Science and Technology, Shizuoka University, July 1999

17) E.W. Peterson, L. Talbot: AIAA J. **8** (1970) 2215

18) F.F. Chen in: Plasma Diagnostic Techniques, eds. R.H. Huddlestone and S.L. Leonard (Academic Press, New York, 1965) p.127

19) V. L. Ginzburg: The Propagation of Electromagnetic Waves in Plasmas (Pergamon Press, Oxford, 1964) p. 260